Analysis, Optimization, and Implementation of Low-Interference Wireless Multicarrier Systems

Gerald Matz, *Member, IEEE,* Dieter Schafhuber, Karlheinz Gröchenig,
Manfred Hartmann, *Student Member, IEEE,* and Franz Hlawatsch, *Senior Member, IEEE*

Abstract— This paper considers pulse-shaping multicarrier (MC) systems that transmit over doubly dispersive fading channels. We provide exact and approximate expressions for the intersymbol and intercarrier interference occurring in such systems. This analysis reveals that the time and frequency concentration of the transmit and receive pulses is of paramount importance for low interference. We prove the (nonobvious) existence of such jointly concentrated pulse pairs by adapting recent mathematical results on Weyl-Heisenberg frames to the MC context. Furthermore, pulse optimization procedures are proposed that aim at low interference and capitalize on the design freedom existing for redundant MC systems. Finally, we present efficient FFT-based modulator and demodulator implementations. Our numerical results demonstrate that for realistic system and channel parameters, optimized pulse-shaping MC systems can outperform conventional cyclic-prefix OFDM systems.

Index Terms— Multicarrier systems, OFDM, doubly dispersive channels, harmonic analysis, pulse design, Weyl-Heisenberg frames.

I. INTRODUCTION

ORTHOGONAL frequency division multiplexing (OFDM) is an attractive multicarrier modulation scheme for broadband wireless communications [1–4]. Conventional OFDM employs rectangular transmit and receive pulses and a cyclic prefix (CP-OFDM) [2]. It is part of, or proposed for, numerous wireless standards like WLANs (IEEE 802.11a,g,n, Hiperlan/2), fixed broadband wireless access (IEEE 802.16), wireless personal area networks (IEEE 802.15), and digital audio and video broadcasting (DAB, DRM, DVB). OFDM is also a promising candidate for future (4G) mobile communication systems.

Recently, *pulse-shaping* OFDM systems and *biorthogonal frequency division multiplexing* (BFDM) systems have attracted increased interest [5–16]. They have several advan-

tages over traditional CP-OFDM systems: higher bandwidth efficiency [5]; reduced sensitivity to carrier frequency offsets, oscillator phase noise, and narrowband interference [6]; and reduced intersymbol/intercarrier interference (ISI/ICI) [5, 15]. In particular, low ISI/ICI will be important for future systems where Doppler frequencies will be larger (equivalently, channel variations will be faster) due to higher carrier frequencies and higher mobile velocities. On the other hand, a drawback of pulse-shaping OFDM/BFDM systems is the potentially poorer peak-to-average power ratio. Furthermore, BFDM systems using a simple equalize-and-slice detector may suffer from noise enhancement since the receive filters are not matched to the transmit filters [5].

While pulse-shaping OFDM systems were proposed rather early [1, 17], only recently the design of the OFDM/BFDM transmit and receive pulses has been considered in more detail. In [18], a pulse-shaping OFDM system using an orthogonalized Gaussian function is proposed and its interference power is analyzed. In [8], a linear combination of Hermite functions is chosen such that orthogonality between neighboring symbols and carriers is obtained. An optimization procedure for OFDM/OQAM (OQAM stands for *offset QAM*) with finitely supported pulses that basically minimizes the out-of-band energy is proposed in [7]; the resulting pulses are linear combinations of prolate spheroidal wave functions. In [9, 12, 13], the duality of multicarrier systems and Weyl-Heisenberg (or Gabor) frames is elaborated and applied to the design of OFDM and BFDM systems. In a similar spirit, [5] proposes an optimization procedure for BFDM systems that builds on frames and Riesz bases and explicitly accounts for channel effects. The time-frequency concentration achievable with Gabor Riesz bases is explored in [19]. In [10], hexagonal time-frequency lattices are advocated, and sphere-packing arguments are used to construct a pulse through orthogonalization of a Gaussian function. The analysis and design of OFDM/OQAM systems using filter bank theory is discussed in [11]. After acceptance for publication of this manuscript, we noticed that similar ideas regarding ISI/ICI analysis and pulse optimization have been developed in [20] (independently of our earlier conference paper [15]).

In this paper, we continue the path taken in [5, 9, 10] and consider the following issues that have not been addressed previously.

- While [5, 9, 10] describe design procedures for OFDM/BFDM systems, no previous theoretical results guaranteed the existence of transmit and receive pulses

that *both* are well concentrated with respect to time and frequency. We settle this issue by using a recent, deep mathematical result from [21] to give explicit expressions for the achievable time and frequency decay of the transmit/receive pulses. This is important because good time-frequency concentration is essential for small ISI/ICI, and because in practice the pulses have to be truncated to finite duration.

- We present an exact ISI/ICI analysis of OFDM/BFDM systems that transmit over time-frequency selective fading channels (previously considered in this context only in [5]). This exact analysis is complemented by new approximate expressions and bounds for the mean ISI/ICI power.

- We propose pulse optimization procedures that use the mean ISI/ICI power as a cost function and thus perform an explicit minimization of ISI/ICI.

- We develop efficient FFT-based implementations of pulse-shaping OFDM/BFDM modulators and demodulators that are only slightly more complex than current CP-OFDM implementations.

- We provide performance evaluations for doubly dispersive fading channels and for realistic spectral efficiencies or, equivalently, redundancies. Previous performance evaluations pertained to spectral efficiencies ≤ 0.5, which are rarely used in practice. Furthermore, apparently for the first time, we compare the performance of pulse-shaping OFDM/BFDM systems with that of standard CP-OFDM systems.

This paper is organized as follows. After a presentation of the multicarrier[1] (MC) system model in Section II, the frame-theoretic computation of biorthogonal pulse pairs is discussed in Section III. In Section IV, it is shown that biorthogonal pulses can have good joint time-frequency concentration. Section V provides an ISI/ICI analysis for MC transmission over doubly dispersive fading channels. In Section VI, we propose two pulse design methods aiming at a minimization of the ISI/ICI power. Efficient FFT-based implementations of the MC modulator and demodulator are developed in Section VII. Finally, Section VIII presents some numerical results.

II. SYSTEM MODEL

A. Modulator and Demodulator

We consider an MC system with K subcarriers, symbol period T, and subcarrier frequency spacing F. The equivalent baseband transmit signal is given by

$$s(t) = \sum_{l=-\infty}^{\infty} \sum_{k=0}^{K-1} a_{l,k}\, g_{l,k}(t)\,. \tag{1}$$

Here, $a_{l,k}$ denotes the data symbol at symbol time $l \in \mathbb{Z}$ and subcarrier $k \in \{0, \ldots, K-1\}$, and

$$g_{l,k}(t) \triangleq g(t-lT)\, e^{j2\pi kF(t-lT)} \tag{2}$$

is a time-frequency (TF) shifted version of the transmit pulse $g(t)$. We assume that the symbols $a_{l,k}$ are i.i.d. with zero mean and mean power $\mathrm{E}\left\{|a_{l,k}|^2\right\} = \sigma_a^2$.

At the receiver, the demodulator computes the inner products of the received signal $r(t)$ with TF shifted versions $\gamma_{l,k}(t) \triangleq \gamma(t-lT)\, e^{j2\pi kF(t-lT)}$ of the receive pulse $\gamma(t)$:[2]

$$x_{l,k} \triangleq \langle r, \gamma_{l,k}\rangle = \int_t r(t)\, \gamma_{l,k}^*(t)\, dt\,. \tag{3}$$

For an ideal channel where $r(t) = s(t)$, perfect demodulation (i.e., $x_{l,k} = a_{l,k}$) is obtained iff the pulses $g(t)$ and $\gamma(t)$ satisfy the *biorthogonality condition*

$$\langle g, \gamma_{l,k}\rangle = \delta_l\,\delta_k\,. \tag{4}$$

For OFDM, we have $\gamma(t) = g(t)$ and thus (4) reduces to the orthogonality condition $\langle g, g_{l,k}\rangle = \delta_l\,\delta_k$.

A necessary condition for (4) is $TF \geq 1$ [22]. Because the spectral efficiency is proportional to $1/(TF)$, the product TF is typically chosen only slightly larger than 1. For practical CP-OFDM systems, TF usually ranges from 1.03 to 1.25, which corresponds to $1/(TF) = 0.8 \ldots 0.97$. A larger value of TF results in a smaller spectral efficiency, but also increases the freedom in designing pulses satisfying (4).

B. Channel

A wireless dispersive fading channel can be modeled as a random time-varying system $\mathbb{H}$ with time-varying impulse response $h(t, \tau)$ [23, 24]. Thus the received signal is given by[3]

$$r(t) = (\mathbb{H}s)(t) = \int_\tau h(t, \tau)\, s(t-\tau)\, d\tau\,. \tag{5}$$

The channel is assumed to satisfy the *wide-sense stationary uncorrelated scattering* (WSSUS) property [23, 24] $\mathrm{E}\left\{h(t, \tau)h^*(t', \tau')\right\} = R_{\mathbb{H}}(t - t', \tau)\, \delta(\tau - \tau')$, where $R_{\mathbb{H}}(\Delta t, \tau)$ is the channel's time-delay correlation function. The second-order statistics of $\mathbb{H}$ can alternatively be described by the *scattering function* defined as [23, 24]

$$C_{\mathbb{H}}(\tau, \nu) = \int_{\Delta t} R_{\mathbb{H}}(\Delta t, \tau)\, e^{-j2\pi\nu\Delta t}\, d\Delta t\,,$$

where ν denotes Doppler frequency. The path gain of the channel is given by $\sigma_{\mathbb{H}}^2 = \int_\tau \int_\nu C_{\mathbb{H}}(\tau, \nu)\, d\tau\, d\nu$. Practical wireless channels are *underspread* [5, 24, 25], i.e., their scattering function is effectively supported within a rectangular region $\mathcal{R} \triangleq [0, \tau_{\max}] \times [-\nu_{\max}, \nu_{\max}]$ of area $2\tau_{\max}\nu_{\max} \ll 1$.

C. Symbol-Level I/O Relation

Combining (1), (3), and (5) yields the following mapping from the transmit symbols $a_{l,k}$ to the receive symbols $x_{l,k}$ [5]:

$$x_{l,k} = \sum_{l'=-\infty}^{\infty} \sum_{k'=0}^{K-1} H_{l,k;l',k'}\, a_{l',k'} \tag{6a}$$

with

$$H_{l,k;l',k'} \triangleq \langle \mathbb{H}g_{l',k'}, \gamma_{l,k}\rangle\,. \tag{6b}$$

The terms in this sum with $(l', k') \neq (l, k)$ describe the ISI and ICI introduced by the channel $\mathbb{H}$. Typically, MC systems are

---

[1]We will use the term "multicarrier" as a unifying term to refer to CP-OFDM, pulse-shaping OFDM, and BFDM.

[2]Integrals are from $-\infty$ to ∞.

[3]Throughout this paper, we consider the noiseless case.

designed such that the ISI/ICI terms in (6) can be neglected, i.e.,

$$x_{l,k} \approx H_{l,k}\, a_{l,k}\,, \qquad (7)$$

with $H_{l,k} \triangleq H_{l,k;l,k}$. This allows the use of a simple scalar equalization at the receiver which, however, suffers from an error floor due to the approximation error associated with (7).

As was observed in [25, 26], the approximate I/O relation (7) means that the transmit pulses $g_{l,k}(t)$ are approximate eigenfunctions of the channel, i.e., $(\mathbb{H}g_{l,k})(t) \approx H_{l,k}\, g_{l,k}(t)$ (together with (4), this implies (7)). This approximation rests crucially on the assumption that the MC pulses are well TF concentrated (cf. Section V). The existence of such pulses will be shown in Section IV.

III. FRAME-THEORETIC COMPUTATION OF MC PULSES

When designing an MC system, a nontrivial task is the construction of transmit and receive pulses with suitable properties. In this section, we show how results from the theory of Weyl-Heisenberg (Gabor) frames can be used to efficiently compute a receive pulse $\gamma(t)$ satisfying the biorthogonality relation (4) for a prescribed transmit pulse $g(t)$. In our discussion, we partly rephrase some ideas from [9, 13].

A. Riesz Sequences, Frames, and Duality Theory

1) Weyl-Heisenberg Riesz Sequences: The biorthogonality condition (4) amounts to the requirement that the transmit symbols $a_{l,k}$ can be uniquely recovered from the transmit signal $s(t)$. This requires that the *Weyl-Heisenberg (WH)* function set $\{g_{l,k}(t)\}$, $(l,k) \in \mathbb{Z}^2$ (cf. (2)) constitutes a *Riesz sequence* [22], i.e., there exist constants $A', B' > 0$ such that[4]

$$A'\|a\|_{\ell^2}^2 \;\leq\; \left\| \sum_{l,k} a_{l,k}\, g_{l,k} \right\|_{L^2}^2 \;\leq\; B'\|a\|_{\ell^2}^2\,, \qquad (8)$$

for all $a_{l,k} \in \ell^2(\mathbb{Z}^2)$. A necessary condition for a WH Riesz sequence is that the TF lattice constants T, F satisfy $TF \geq 1$. If $\{g_{l,k}(t)\}$ is a WH Riesz sequence, there exists a (generally nonunique) WH Riesz sequence $\{\gamma_{l,k}(t)\}$ that satisfies the biorthogonality condition (4) and allows one to recover the transmit symbols $a_{l,k}$ according to (3) (with $r(t) = s(t)$).

If $\langle g, g_{l,k}\rangle = \delta_l\, \delta_k$ holds in addition to (8), then the Riesz sequence $\{g_{l,k}(t)\}$ is an *orthogonal* sequence that corresponds to a pulse-shaping OFDM (and not just BFDM) system.

2) Weyl-Heisenberg (Gabor) Frames: We now consider a different concept whose relation to WH Riesz sequences will be discussed presently. A WH function set $\{\widetilde{g_{l,k}}(t)\}$, $(l,k) \in \mathbb{Z}^2$, with $\widetilde{g_{l,k}}(t) = g(t - l\tilde{T})\, e^{j2\pi k \tilde{F} t}$ is called a *WH frame* [22] if there exist constants $A, B > 0$ (the *frame bounds*) such that

$$A\|x\|_{L_2}^2 \;\leq\; \sum_{l,k} |\langle x, \widetilde{g_{l,k}}\rangle|^2 \;\leq\; B\|x\|_{L_2}^2\,, \qquad (9)$$

for all $x(t) \in L_2(\mathbb{R})$. The frame property (9) means that $x(t)$ is completely and stably determined by the frame coefficients $\langle x, \widetilde{g_{l,k}}\rangle$ via the *frame expansion* $x(t) = \sum_{l,k} \langle x, \widetilde{g_{l,k}}\rangle\, \widetilde{\gamma_{l,k}}(t)$ that involves a (generally nonunique) *dual pulse* $\gamma(t)$. A necessary condition for WH frames is $\tilde{T}\tilde{F} \leq 1$ (note the difference from WH Riesz sequences that require $\tilde{T}\tilde{F} \geq 1$). If the frame bounds coincide ($A = B$), then $\{\widetilde{g_{l,k}}(t)\}$ is called a *tight* WH frame. In this case $\gamma(t) = \frac{\tilde{T}\tilde{F}}{A}\, g(t)$, i.e., the dual pulse equals the original pulse up to a constant factor.

3) Ron-Shen Duality: WH frames and WH Riesz sequences are related by the *Ron-Shen duality theorem* that is stated as follows [27, 28]. Let $\{g_{l,k}(t)\}$ and $\{\gamma_{l,k}(t)\}$ be WH sets on the lattice (T, F), and let $\{\widetilde{g_{l,k}}(t)\}$ and $\{\widetilde{\gamma_{l,k}}(t)\}$ be the corresponding WH sets on the *adjoint lattice* $(\tilde{T}, \tilde{F}) = (1/F, 1/T)$. Then

- $\{g_{l,k}(t)\}$ is a Riesz sequence iff $\{\widetilde{g_{l,k}}(t)\}$ is a frame;
- $\{g_{l,k}(t)\}$ and $\{\gamma_{l,k}(t)\}$ are biorthogonal Riesz sequences iff $\{\widetilde{g_{l,k}}(t)\}$ and $\{\widetilde{\gamma_{l,k}}(t)\}$ are dual frames;
- $\{g_{l,k}(t)\}$ is an orthogonal Riesz sequence iff $\{\widetilde{g_{l,k}}(t)\}$ is a tight frame.

B. Application to Pulse Computation

Based on the above duality relation, the computation of pulses inducing (bi)orthogonal WH Riesz sequences can be reduced to the computation of *dual WH frames on the adjoint lattice*, for which frame-theoretic methods are available (cf. [22, 29]). We thus obtain the following procedure.

1) Choose lattice constants T, F and a pulse $g(t)$ such that the WH set $\{\widetilde{g_{l,k}}(t)\}$ on the adjoint lattice $(\tilde{T}, \tilde{F}) = (1/F, 1/T)$ is a WH frame (this requires $TF \geq 1$). We note that if $g(t)$ is bounded and vanishes outside $[0, T']$ with $1/F \leq T' \leq T$, then $\{\widetilde{g_{l,k}}(t)\}$ is a WH frame iff

$$a \;\leq\; \sum_k \left| g\!\left(t - \frac{k}{F}\right) \right|^2 \;\leq\; b \qquad (10)$$

with some $a, b > 0$ [22]. In particular, $\{\widetilde{g_{l,k}}(t)\}$ is a tight WH frame iff the above condition holds with $a = b$, i.e., iff $\sum_k |g(t - \frac{k}{F})|^2 = \text{const}$.

2a) For a BFDM system, the $g(t)$ chosen in 1) is used as the transmit pulse, and the minimum L^2-norm biorthogonal receive pulse $\gamma(t)$ is given by the *canonical dual pulse* defined by the equation

$$\frac{1}{TF}\, (\tilde{\mathbb{S}}\gamma)(t) = g(t)\,. \qquad (11)$$

Here, $\tilde{\mathbb{S}}$ is the *frame operator* defined by

$$(\tilde{\mathbb{S}}x)(t) = \sum_{l,k} \langle x, \widetilde{g_{l,k}}\rangle\, \widetilde{g_{l,k}}(t)\,.$$

2b) For an OFDM system, the transmit and receive pulses are both given by the function $g^\perp(t)$ that is the solution of

$$\frac{1}{\sqrt{TF}}\, (\tilde{\mathbb{S}}^{1/2} g^\perp)(t) = g(t)\,, \qquad (12)$$

where $\tilde{\mathbb{S}}^{1/2}$ is the positive definite square root of the frame operator $\tilde{\mathbb{S}}$.

The operators $\tilde{\mathbb{S}}$ and $\tilde{\mathbb{S}}^{1/2}$ are invertible, and thus (11) and (12) have unique solutions that can be written as $\gamma(t) =$

---

[4]The subsequent development applies to an infinite number of subcarriers; the results so obtained are representative if the actual number of subcarriers is reasonably large. The squared ℓ^2-norm of a sequence $a_{l,k}$ is $\|a\|_{\ell^2}^2 = \sum_{l,k} |a_{l,k}|^2$ and the squared L^2-norm of a signal $s(t)$ is $\|s\|_{L^2}^2 = \int_t |s(t)|^2\, dt$. Summations are from $-\infty$ to ∞ unless indicated otherwise.

$TF(\tilde{\mathbb{S}}^{-1}g)(t)$ and $g^{\perp}(t) = \sqrt{TF}(\tilde{\mathbb{S}}^{-1/2}g)(t)$, respectively. For an efficient numerical solution, conjugate gradient and matrix factorization methods [29] as well as Zak transform methods [9, 13] are available. Alternatively, $\gamma(t)$ can be computed by inserting the expansion $\gamma(t) = \sum_{l,k} c_{l,k}\, g_{l,k}(t)$ into the biorthogonality condition (4), which yields a linear equation in the unknown coefficients $c_{l,k}$ [29].

For given $g(t)$ and $TF > 1$, there exists a whole affine space of biorthogonal pulses. These are all of the form $\gamma'(t) = \gamma(t) + \psi(t)$ where $\gamma(t)$ is the canonical biorthogonal pulse as defined by (11) and $\psi(t)$ is an arbitrary function in the orthogonal complement of $\mathcal{G} \triangleq \mathrm{span}\{g_{l,k}(t)\}$ [22]. This fact leads to a design freedom that can be exploited for system optimization (see Section VI).

IV. TIME-FREQUENCY CONCENTRATION OF MC PULSES

The foregoing discussion has shown how the canonical biorthogonal pulse $\gamma(t)$ and the orthogonalized pulse $g^{\perp}(t)$ can be constructed for a given transmit pulse $g(t)$. However, when a $g(t)$ with good TF concentration is chosen, it is not clear *a priori* if $\gamma(t)$ and $g^{\perp}(t)$ have good TF concentration as well. We now answer this question by using a recent mathematical result [21] to show that the canonical $\gamma(t)$ in (11) and the orthogonalized pulse $g^{\perp}(t)$ in (12) inherit the TF localization properties of $g(t)$. This is practically important because the ISI/ICI in the case of doubly dispersive channels is determined by the joint TF concentration of $g(t)$ and $\gamma(t)$. More specifically, we will show in Section V that the ISI/ICI power depends on the cross-ambiguity function (CAF) of $\gamma(t)$ and $g(t)$ that is defined as $A_{\gamma,g}(\tau,\nu) \triangleq \int_t \gamma(t)\, g^*(t-\tau)\, e^{-j2\pi\nu t} dt$ [22]. Therefore, we will use the CAF as a measure of the TF concentration of pulses. We note that for rational TF, temporal and spectral decay properties of the canonical dual pulse and of the orthogonalized pulse have been proved using weighted L_1 spaces in [19].

A. TF Localization of (Bi)orthogonal Pulses

We will say that a pulse $g(t)$ is *polynomially localized* of degree $s \geq 0$ if

$$\int_\tau \int_\nu |A_{g,g}(\tau,\nu)| \left(1 + \left|\frac{\tau}{T_0}\right| + |\nu T_0|\right)^s d\tau\, d\nu \;<\; \infty\,,$$

with an arbitrary normalization time constant $T_0 > 0$. This condition implies that $|A_{g,g}(\tau,\nu)| \leq c \left(1 + \left|\frac{\tau}{T_0}\right| + |\nu T_0|\right)^{-s}$ with some $c > 0$ and that all moments of $A_{g,g}(\tau,\nu)$ up to order s are finite, i.e., $\int_\tau \int_\nu |A_{g,g}(\tau,\nu)| \left|\frac{\tau}{T_0}\right|^m |\nu T_0|^n d\tau\, d\nu < \infty$ for $m+n \leq s$. An even stronger concept of TF localization is obtained by replacing $\left(1 + \left|\frac{\tau}{T_0}\right| + |\nu T_0|\right)^s$ by the sub-exponential weight $e^{b(|\tau/T_0|+|\nu T_0|)^\beta}$ with $b > 0$ and $0 < \beta < 1$. We say that $g(t)$ is *sub-exponentially localized* if

$$\int_\tau \int_\nu |A_{g,g}(\tau,\nu)|\, e^{b(|\tau/T_0|+|\nu T_0|)^\beta} d\tau\, d\nu \;<\; \infty\,.$$

This condition implies that $|A_{g,g}(\tau,\nu)| \leq c\, e^{-b(|\tau/T_0|+|\nu T_0|)^\beta}$ and that *all* moments of $A_{g,g}(\tau,\nu)$ are finite.

Our main theoretical result asserts the existence of transmit and receive pulses that *simultaneously* have excellent TF concentration properties.

Localization Theorem. Assume that $\{\widetilde{g_{l,k}}(t)\}$, $(l,k) \in \mathbb{Z}^2$, with $\widetilde{g_{l,k}}(t) = g(t - l/F)\, e^{j2\pi kt/T}$ is a WH frame.

(a) If $g(t)$ is polynomially localized of degree s, then the canonical biorthogonal pulse $\gamma(t) = TF(\tilde{\mathbb{S}}^{-1}g)(t)$ and the orthogonalized pulse $g^{\perp}(t) = \sqrt{TF}(\tilde{\mathbb{S}}^{-1/2}g)(t)$ are also polynomially localized of degree s, and furthermore the CAF of $\gamma(t), g(t)$ satisfies

$$\int_\tau \int_\nu |A_{\gamma,g}(\tau,\nu)| \left(1 + \left|\frac{\tau}{T_0}\right| + |\nu T_0|\right)^s d\tau\, d\nu \;<\; \infty\,. \tag{13}$$

(b) If $g(t)$ is sub-exponentially localized, then $\gamma(t)$ and $g^{\perp}(t)$ are also sub-exponentially localized (with the same constants b,β), and the CAF of $\gamma(t), g(t)$ satisfies

$$\int_\tau \int_\nu |A_{\gamma,g}(\tau,\nu)|\, e^{b(|\tau/T_0|+|\nu T_0|)^\beta} d\tau\, d\nu \;<\; \infty\,. \tag{14}$$

The proof of this theorem (not included here) is an application of [21] in combination with Ron-Shen duality theory. We note that this result agrees well with previous empirical observations reported in [9].

B. Examples

1) Spline-type Pulse: Choose $T_1, \ldots, T_n > 0$ and construct the transmit pulse as $g(t) = (\chi_1 * \cdots * \chi_n)(t)$, where $\chi_k(t) = 1$ for $t \in (-T_k/2, T_k/2)$ and 0 otherwise, and $*$ denotes convolution. Then $g(t) = 0$ for $|t| \geq \frac{1}{2}\sum_{k=1}^n T_k$. By construction, $A_{g,g}(\tau,\nu) = 0$ for $|\tau| \geq \frac{1}{2}\sum_{k=1}^n T_k$. For $|\tau| < \frac{1}{2}\sum_{k=1}^n T_k$, it can be shown that $|A_{g,g}(\tau,\nu)| \leq c(1 + |\nu|)^{-n+1}$. Hence, $g(t)$ is polynomially localized of degree $s = n-1$. If $\{\widetilde{g_{l,k}}(t)\}$ is a WH frame (which can be checked by means of (10)), our localization theorem guarantees that the canonical biorthogonal receive pulse $\gamma(t)$ is also polynomially localized and that (13) holds.

2) Gaussian Pulse: The transmit pulse with best TF localization is the Gaussian pulse $g(t) = e^{-\pi(t/T_0)^2}$. Its ambiguity function is $A_{g,g}(\tau,\nu) = e^{-\frac{\pi}{2}[(\tau/T_0)^2+(\nu T_0)^2]}$, and thus $g(t)$ is sub-exponentially localized for *all* $b > 0$, $\beta < 1$. Furthermore $\{\widetilde{g_{l,k}}(t)\}$ is a WH frame iff $TF > 1$ [22, 30]. By our localization theorem, the canonical $\gamma(t)$ is then also sub-exponentially localized for all $b > 0$, $\beta < 1$; moreover, (14) holds for all $b > 0$, $\beta < 1$.

V. INTERFERENCE ANALYSIS

In this section, we provide a detailed ISI/ICI analysis of pulse-shaping MC systems transmitting over a WSSUS channel (for the special case of CP-OFDM see [31]). For simplicity, we assume an infinite number of subcarriers. Parts of the results below have previously been obtained in [5].

A. Exact Analysis

We define the *mean ISI/ICI power* as the mean-square error of the approximation (7):

$$\sigma_{\mathrm{I}}^2 \triangleq \mathrm{E}\{|x_{l,k} - H_{l,k}\, a_{l,k}|^2\}\,.$$

Using the statistical independence of the symbols $a_{l,k}$, one obtains $\sigma_{\mathrm{I}}^2 = \sigma_x^2 - \sigma_{\mathrm{D}}^2$, where $\sigma_x^2 \triangleq \mathrm{E}\{|x_{l,k}|^2\}$ is the total received power and $\sigma_{\mathrm{D}}^2 \triangleq \mathrm{E}\{|H_{l,k}\, a_{l,k}|^2\}$ is the power of the

desired component (σ_{I}^2 and σ_{D}^2 do not depend on l and k since the channel is assumed WSSUS). Further using the WSSUS assumption, one can show that

$$\sigma_{\mathrm{D}}^2 = \sigma_a^2 \int_\tau \int_\nu C_{\mathbb{H}}(\tau,\nu) \, |A_{\gamma,g}(\tau,\nu)|^2 \, d\tau \, d\nu. \qquad (15)$$

If $|A_{\gamma,g}(\tau,\nu)|^2 \approx 1$ on the effective support of the scattering function $C_{\mathbb{H}}(\tau,\nu)$, then $\sigma_{\mathrm{D}}^2 \approx \sigma_a^2 \, \sigma_{\mathbb{H}}^2$. We note that (4) implies $A_{\gamma,g}(0,0) = 1$, i.e., at the origin $A_{\gamma,g}(\tau,\nu)$ is exactly equal to 1. Similarly, one can show

$$\sigma_x^2 = \sigma_a^2 \int_\tau \int_\nu C_{\mathbb{H}}(\tau,\nu) \, P_{\gamma,g}(\tau,\nu) \, d\tau \, d\nu, \qquad (16a)$$

with

$$P_{\gamma,g}(\tau,\nu) \triangleq \sum_{l,k} |A_{\gamma,g}(\tau-lT,\nu-kF)|^2. \qquad (16b)$$

Inserting (15) and (16) into $\sigma_{\mathrm{I}}^2 = \sigma_x^2 - \sigma_{\mathrm{D}}^2$, we finally obtain the following delay-Doppler domain expression of the ISI/ICI power:

$$\sigma_{\mathrm{I}}^2 = \sigma_a^2 \int_\tau \int_\nu C_{\mathbb{H}}(\tau,\nu) \, P_{\gamma,g}^{(0)}(\tau,\nu) \, d\tau \, d\nu, \qquad (17)$$

where $P_{\gamma,g}^{(0)}(\tau,\nu)$ is a periodized version of $|A_{\gamma,g}(\tau,\nu)|^2$ with the term $|A_{\gamma,g}(\tau,\nu)|^2$ itself suppressed, i.e.,

$$P_{\gamma,g}^{(0)}(\tau,\nu) \triangleq P_{\gamma,g}(\tau,\nu) - |A_{\gamma,g}(\tau,\nu)|^2$$
$$= \sum_{(l,k)\neq(0,0)} |A_{\gamma,g}(\tau-lT,\nu-kF)|^2.$$

Let $\mathcal{R} = [0, \tau_{\max}] \times [-\nu_{\max}, \nu_{\max}]$ denote the effective support of $C_{\mathbb{H}}(\tau,\nu)$. According to (17), σ_{I}^2 will be small for small overlap of $C_{\mathbb{H}}(\tau,\nu)$ with $|A_{\gamma,g}(\tau-lT, \nu-kF)|$, $(l,k) \neq (0,0)$, which in turn requires that $|A_{\gamma,g}(\tau,\nu)|^2$ is small within all regions $[lT, lT + \tau_{\max}] \times [kF - \nu_{\max}, kF + \nu_{\max}]$, $(l,k) \neq (0,0)$ (note that the biorthogonality relation (4) implies $A_{\gamma,g}(lT, kF) = 0$ for $(l,k) \neq (0,0)$). This can be achieved if $A_{\gamma,g}(\tau,\nu)$ decays sufficiently fast outside the support region $\mathcal{R}$ of $C_{\mathbb{H}}(\tau,\nu)$, which is facilitated if $\mathcal{R}$ is small (i.e., the channel is weakly dispersive) and the lattice constants T and F are large. Since large T and F entails poor spectral efficiency and the channel dispersion is beyond the control of the designer, it is crucial to design pulses $g(t)$ and $\gamma(t)$ that are *jointly* well TF concentrated such that their CAF decays quickly. The existence of such pulse pairs was established by our localization theorem in Section IV. We conclude that, with regard to practical design, excellent joint TF concentration of the transmit and receive pulses is the most important requirement for low ISI/ICI.

B. Approximations and Bounds

Sometimes the channel's second-order statistics (scattering function $C_{\mathbb{H}}(\tau,\nu)$) are not known exactly, and thus the ISI/ICI power σ_{I}^2 cannot be determined according to (17). In such situations, we need approximations of σ_{I}^2 in terms of more readily available global channel parameters.

The underspread assumption means that $C_{\mathbb{H}}(\tau,\nu)$—and, thus, the integrand in (17)—is effectively zero outside the support region $\mathcal{R}$ of area $\ll 1$. Within this region, $|A_{\gamma,g}(\tau,\nu)|^2$

can be well approximated by its second-order Taylor expansion (cf. [32]). Without loss of generality, we assume that $|\langle g, \gamma \rangle|^2 \equiv |A_{\gamma,g}(0,0)|^2 = 1$. Furthermore, to obtain simpler and more intuitive results, we restrict to real-valued and even transmit and receive pulses. This restriction causes the first-order and mixed derivatives in the second-order Taylor expansion to vanish. We thus obtain the approximation

$$|A_{\gamma,g}(\tau,\nu)|^2 \approx 1 + \frac{\tau^2}{2} \left[\frac{\partial^2}{\partial\tau^2} |A_{\gamma,g}(\tau,\nu)|^2 \right]_{(0,0)}$$
$$+ \frac{\nu^2}{2} \left[\frac{\partial^2}{\partial\nu^2} |A_{\gamma,g}(\tau,\nu)|^2 \right]_{(0,0)}$$
$$= 1 - 2\pi^2 \left(\tau^2 B_{g,\gamma} + \nu^2 D_{g,\gamma} \right), \qquad (18)$$

where

$$D_{g,\gamma} \triangleq \int_t t^2 \, g(t) \, \gamma(t) \, dt, \qquad B_{g,\gamma} \triangleq \int_f f^2 \, G(f) \, \Gamma(f) \, df$$

are measures of the "joint" duration and bandwidth, respectively, of $g(t), \gamma(t)$. Inserting (18) into (17), we obtain the desired approximation for the ISI/ICI power as

$$\sigma_{\mathrm{I}}^2 \approx \sigma_a^2 (\eta_1 + \eta_2), \qquad (19)$$

with

$$\eta_1 \triangleq 2\pi^2 \sigma_{\mathbb{H}}^2 \left(\sigma_\tau^2 B_{g,\gamma} + \sigma_\nu^2 D_{g,\gamma} \right),$$
$$\eta_2 \triangleq \int_\tau \int_\nu C_{\mathbb{H}}(\tau,\nu) \left[P_{\gamma,g}(\tau,\nu) - 1 \right] d\tau \, d\nu.$$

Here σ_τ^2 and σ_ν^2 denote the channel's delay spread and Doppler spread, respectively:

$$\sigma_\tau^2 \triangleq \frac{1}{\sigma_{\mathbb{H}}^2} \int_\tau \int_\nu \tau^2 \, C_{\mathbb{H}}(\tau,\nu) \, d\tau \, d\nu,$$
$$\sigma_\nu^2 \triangleq \frac{1}{\sigma_{\mathbb{H}}^2} \int_\tau \int_\nu \nu^2 \, C_{\mathbb{H}}(\tau,\nu) \, d\tau \, d\nu.$$

The quantity η_1 is a measure of the "joint" TF concentration of $g(t), \gamma(t)$ relative to the channel dispersion parameters σ_τ^2 and σ_ν^2. Note that η_1 is determined by the decay of $A_{\gamma,g}(\tau,\nu)$, which underlines the practical relevance of our localization theorem in Section IV. The second quantity, η_2, is a (channel-dependent) measure of how much the pulses $g(t), \gamma(t)$ deviate from the OFDM case. This interpretation is motivated by the fact that for critically sampled OFDM systems—i.e., for $TF = 1$, $\gamma(t) = g(t)$ and $\langle g, g_{l,k} \rangle = \delta_l \delta_k$—one has $P_{g,g}(\tau,\nu) \equiv 1$ [33] and consequently $\eta_2 = 0$. We conclude that for a BFDM system, the ISI/ICI power is determined by the joint TF concentration of the transmit and receive pulses (as expressed by η_1) and the deviation from orthogonality (as expressed by η_2). Thus, for low interference, the pulses should be jointly well localized in time and frequency and close to an orthogonal system.

If $C_{\mathbb{H}}(\tau,\nu)$ is supported within $\mathcal{R} = [0, \tau_{\max}] \times [-\nu_{\max}, \nu_{\max}]$, one can derive the upper bounds

$$\eta_1 \leq 2\pi^2 \sigma_{\mathbb{H}}^2 \left(\tau_{\max}^2 B_{g,\gamma} + \nu_{\max}^2 D_{g,\gamma} \right),$$
$$\eta_2 \leq \sigma_{\mathbb{H}}^2 \max_{(\tau,\nu)\in\mathcal{R}} \left[P_{\gamma,g}(\tau,\nu) - 1 \right].$$

These bounds involve the maximum delay $\tau_{\max}$ and the maximum Doppler frequeny $\nu_{\max}$, which may be more readily available than σ_τ^2 and σ_ν^2.

For a conventional CP-OFDM system with cyclic-prefix length $T_{cp} > \tau_{max}$ (i.e., no ISI), it can be shown that (19) simplifies to $\sigma_I^2 \approx \frac{\pi^2}{3} \sigma_a^2 \sigma_{\mathbb{H}}^2 \sigma_\nu^2 (T - T_{cp})^2$. This expression generalizes results previously obtained for Jakes and uniform Doppler spectra [31] and for "frequency offset" channels [34].

VI. PULSE OPTIMIZATION

We have seen that for low ISI/ICI, an MC system should be almost orthogonal and use pulses that are jointly well localized in time and frequency. Our localization theorem shows that such well-localized pulse pairs exist: for a given transmit pulse with polynomial (sub-exponential) TF localization, the *canonical* biorthogonal receive pulse also has polynomial (sub-exponential) TF localization and the CAF of the two pulses decays fast. However, for $TF > 1$ there are other biorthogonal receive pulses besides the canonical one. We next propose a pulse optimization procedure that exploits this design freedom to improve on the canonical biorthogonal receive pulse in terms of ISI/ICI. We also propose a numerical optimization that dispenses with the biorthogonality constraint to achieve a further reduction of ISI/ICI. The symbol period T and subcarrier spacing F will be assumed fixed. In practice, based on the prior choice of the product TF as dictated by the spectral efficiency to be achieved, the values of T and F should be chosen by means of the rule of thumb [5, 18] $T/F = \sqrt{\sigma_\tau^2/\sigma_\nu^2}$ (or $T/F = \tau_{max}/(2\nu_{max})$ if σ_τ^2 and σ_ν^2 are unknown).

A. Linear Optimization

Our first pulse optimization method uses a prescribed transmit pulse $g^{(0)}(t)$ and calculates the receive pulse $\gamma(t)$ minimizing the ISI/ICI power σ_I^2 subject to the biorthogonality condition (4). For fixed $g^{(0)}(t)$ and $TF > 1$, any biorthogonal receive pulse $\gamma(t)$ can be written as [22]

$$\gamma(t) = \gamma^{(0)}(t) + \psi(t). \tag{20}$$

Here, $\gamma^{(0)}(t)$ is the canonical biorthogonal pulse associated to $g^{(0)}(t)$ and $\psi(t)$ is an arbitrary element of the orthogonal complement space $\mathcal{G}^\perp$ of $\mathcal{G} = \text{span}\{g_{l,k}^{(0)}(t)\}$, i.e., $\langle \psi, g_{l,k}^{(0)} \rangle = 0$ for all l, k. Hence, $\psi(t)$ can be written as $\psi(t) = \sum_i c_i u_i(t)$ where $\{u_i(t)\}$ is an orthonormal basis of $\mathcal{G}^\perp$ and $c_i = \langle \psi, u_i \rangle$ denotes the corresponding coefficient of $\psi(t)$. Using (20), the minimization of σ_I^2 with respect to $\gamma(t)$ under the biorthogonality constraint (4) can be formulated as an *unconstrained* minimization with respect to the coefficients c_i.

It will be convenient to use the following expression for σ_I^2 that is equivalent to (17) (cf. [5]):

$$\sigma_I^2 = \sigma_a^2 \int_\tau \int_\nu Q_{\mathbb{H}}^{(0)}(\tau, \nu) |A_{\gamma,g}(\tau, \nu)|^2 d\tau d\nu, \tag{21}$$

where

$$Q_{\mathbb{H}}^{(0)}(\tau, \nu) \triangleq \sum_{(l,k) \neq (0,0)} C_{\mathbb{H}}(\tau - lT, \nu - kF)$$

is a periodized version of $C_{\mathbb{H}}(\tau, \nu)$ with the term at the origin suppressed. Inserting (20) in (21), it is seen that σ_I^2 depends

quadratically on the coefficients c_i. The (unconstrained) minimization of σ_I^2 with respect to the c_i's then amounts to solving the linear equation[5] $\mathbf{B}\mathbf{c} = -\mathbf{b}$ with $[\mathbf{c}]_i = c_i$ and

$$[\mathbf{B}]_{i,j} = \int_\tau \int_\nu Q_{\mathbb{H}}^{(0)}(\tau, \nu) A_{u_i, g^{(0)}}^*(\tau, \nu) A_{u_j, g^{(0)}}(\tau, \nu) d\tau d\nu,$$

$$[\mathbf{b}]_i = \int_\tau \int_\nu Q_{\mathbb{H}}^{(0)}(\tau, \nu) A_{u_i, g^{(0)}}^*(\tau, \nu) A_{\gamma^{(0)}, g^{(0)}}(\tau, \nu) d\tau d\nu.$$

Thus the optimal biorthogonal receive pulse associated to the given transmit pulse $g^{(0)}(t)$ is obtained as

$$\gamma^{opt}(t) = \gamma^{(0)}(t) + \sum_i c_i^{opt} u_i(t) \quad \text{with} \quad \mathbf{c}^{opt} = -\mathbf{B}^{-1}\mathbf{b}. \tag{22}$$

The same approach can be used to optimize the transmit pulse $g(t)$ for a prescribed receive pulse $\gamma^{(0)}(t)$.

The optimal pulse resulting from this design method depends on the channel statistics (scattering function $C_{\mathbb{H}}(\tau, \nu)$). If the scattering function is not known or if good pulses are desired for a broad range of channel statistics, one may use by default the brick-shaped scattering function

$$C_{\mathbb{H}}(\tau, \nu) = \begin{cases} \frac{\sigma_{\mathbb{H}}^2}{2\tau_{max}\nu_{max}}, & (\tau, \nu) \in \mathcal{R} \\ 0, & (\tau, \nu) \notin \mathcal{R}, \end{cases} \tag{23}$$

with a suitable (worst-case) choice of τ_{max} and ν_{max}.

The pulse pair $g^{(0)}(t), \gamma^{opt}(t)$ may be quite different from an orthogonal system. Near-orthogonality, which is desirable for low ISI/ICI (cf. Section V-B) and for low noise after demodulation, can be obtained by the following iterative extension of our pulse optimization method. The optimal receive pulse $\gamma^{opt}(t)$ is "orthogonalized" according to (12) (with $g(t)$ replaced by $\gamma^{opt}(t)$). Subsequently, a new optimization run is performed to compute the optimal biorthogonal transmit pulse associated to the orthogonalized receive pulse. The resulting pulse is again orthogonalized, etc.

B. Joint Nonlinear Optimization

The linear optimization method discussed above has the drawback that one of the two pulses must be chosen beforehand and is not optimized. Therefore, we next propose a *joint* optimization of $g(t)$ and $\gamma(t)$. As a cost function, we use the reciprocal of the signal-to-interference ratio (SIR) σ_D^2/σ_I^2,

$$J(g, \gamma) \triangleq \frac{\sigma_I^2}{\sigma_D^2} = \frac{\int_\tau \int_\nu Q_{\mathbb{H}}^{(0)}(\tau, \nu) |A_{\gamma, g}(\tau, \nu)|^2 d\tau d\nu}{\int_\tau \int_\nu C_{\mathbb{H}}(\tau, \nu) |A_{\gamma, g}(\tau, \nu)|^2 d\tau d\nu} \tag{24}$$

(cf. (15), (21)). The goal is to minimize $J(g, \gamma)$ simultaneously with respect to $g(t)$ and $\gamma(t)$. For the sake of increased design freedom, we perform this minimization without the biorthogonality constraint (4). Thus, the resulting pulses are not necessarily exactly biorthogonal. While this allows for lower ISI/ICI power in the case of dispersive channels, there will be some residual ISI/ICI—typically below the noise level—for an ideal (nondispersive) channel. However, this is not a problem because an ideal channel rarely occurs in practice. Moreover, we observed that the jointly optimized pulses tend to be almost biorthogonal (in fact, almost orthogonal).

---

[5]In practical digital implementations, the matrix $\mathbf{B}$ and the vectors $\mathbf{b}$ and $\mathbf{c}$ are finite-dimensional.
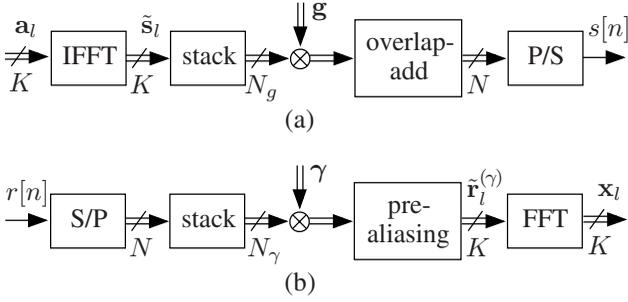
Fig. 1. *Efficient implementation of pulse-shaping MC systems: (a) Modulator, (b) demodulator.*

The minimization of $J(g, \gamma)$ has to be done by means of numerical techniques. We used the unconstrained minimization function *fminunc* from MATLAB's optimization toolbox [35]. In general, the resulting pulses correspond to a local minimum of $J(g, \gamma)$, and they depend on the pulses used for initializing the minimization procedure.

VII. EFFICIENT IMPLEMENTATION

Practical application of pulse-shaping MC systems requires efficient digital implementations of the modulator and demodulator. In this section, we propose overlap-add type implementations for rational TF that are motivated by filterbank theory [36]. (We note that direct polyphase implementations [36] are problematic because they require TF to be integer whereas actually $1 < TF < 2$.) The sampling rate used for discretizing all signals is chosen equal to the system bandwidth KF. In the resulting discrete-time setting, the subcarrier spacing is $1/K$ and the discrete symbol period is $N = KTF$. The sampled transmit pulse $g[n]$ and receive pulse $\gamma[n]$ are assumed to have finite support $[-N_1^{(g)}, N_2^{(g)}]$ and $[-N_1^{(\gamma)}, N_2^{(\gamma)}]$ respectively. Their respective duration is thus given by $N_g = N_1^{(g)} + N_2^{(g)} + 1$ and $N_\gamma = N_1^{(\gamma)} + N_2^{(\gamma)} + 1$.

The proposed efficient implementations of the pulse-shaping MC modulator and demodulator are depicted in Fig. 1. They combine the length-K IFFT or FFT used by conventional CP-OFDM systems with a pulse-shaping operation (elementwise multiplication by the vector $\mathbf{g} = (g[-N_1^{(g)}] \cdots g[N_2^{(g)}])^T$ or $\boldsymbol{\gamma} = (\gamma[-N_1^{(\gamma)}] \cdots \gamma[N_2^{(\gamma)}])^T$) and with an overlap-add or pre-aliasing operation.

A. Modulator

The digital modulator computes the transmit signal (cf. (1))

$$s[n] = \frac{1}{\sqrt{K}} \sum_{l=-\infty}^{\infty} \sum_{k=0}^{K-1} a_{l,k} \, g[n - lN] \, e^{j2\pi \frac{k}{K}(n-lN)} \, .$$

Due to the finite length of $g[n]$, within the lth symbol period $s[n]$ can be written as

$$s[n] = \sum_{i=l-L_2^{(g)}}^{l+L_1^{(g)}} s_i^{(g)}[n-iN], \quad n \in [lN, (l+1)N-1], \quad (25)$$

where $L_1^{(g)} = \lceil (N_1^{(g)} - 1)/N \rceil$, $L_2^{(g)} = \lfloor N_2^{(g)}/N \rfloor$, and the partial transmit signals $s_l^{(g)}[n]$ are obtained by windowing the

IDFT of the transmit symbols $a_{l,k}$:

$$s_l^{(g)}[n] = \tilde{s}_l[n] g[n], \quad \text{with } \tilde{s}_l[n] = \frac{1}{\sqrt{K}} \sum_{k=0}^{K-1} a_{l,k} \, e^{j2\pi \frac{nk}{K}}. \tag{26}$$

Equation (25) describes an overlap-add operation that involves $L_1^{(g)} + L_2^{(g)} + 1$ windowed IDFT signals $s_i^{(g)}[n]$ as given by (26). We note that $L_1^{(g)} + L_2^{(g)} + 1$ is essentially the number of overlapping transmit pulses, which typically is less than 5. The signals $s_i^{(g)}[n]$ can be computed as follows. First, the vector $\tilde{\mathbf{s}}_l = (\tilde{s}_l[0] \cdots \tilde{s}_l[K-1])^T$ containing the length-K IDFT of the lth block of transmit symbols $a_{l,k}$, $k = 0, \ldots, K-1$, is repeatedly stacked to form a vector of length N_g. Subsequently, this longer vector is multiplied elementwise by the transmit pulse vector $\mathbf{g}$. These operations are depicted in Fig. 1(a).

B. Demodulator

At the receiver, the received signal $r[n]$ is demodulated according to (cf. (3))

$$x_{l,k} = \frac{1}{\sqrt{K}} \sum_{n=-\infty}^{\infty} r[n] \, \gamma^*[n - lN] \, e^{-j2\pi \frac{k}{K}(n-lN)} \, .$$

The summation is actually finite due to the finite length of $\gamma[n]$. The above expression can be efficiently implemented by means of the length-K normalized DFT

$$x_{l,k} = \frac{1}{\sqrt{K}} \sum_{n=0}^{K-1} \tilde{r}_l^{(\gamma)}[n] \, e^{-j2\pi \frac{kn}{K}} \, .$$

Here, the lth length-K receive block $\tilde{r}_l^{(\gamma)}[n]$ is obtained through windowing and "pre-aliasing" operations, i.e.,

$$\tilde{r}_l^{(\gamma)}[n] = \sum_{i=-L_2^{(\gamma)}}^{L_1(\gamma)} r_l^{(\gamma)}[n-iK], \quad \text{with } r_l^{(\gamma)}[n] = r[n+lN] \, \gamma^*[n],$$

where $L_1^{(\gamma)} = \lceil (N_1^{(\gamma)} - 1)/K \rceil$ and $L_2(\gamma) = \lfloor N_2^{(\gamma)}/K \rfloor$. Again, $L_1^{(\gamma)} + L_2^{(\gamma)} + 1$ is the number of overlapping receive pulses, with typical values less than 5. The resulting demodulator implementation is shown in Fig. 1(b).

C. Computational Complexity

The computational complexity of the modulator is dominated by the IDFT and pulse shaping in (26), which require about $\mathcal{O}(K \log K + N_g)$ operations per symbol. Similarly, at the demodulator the DFT and windowing amount to $\mathcal{O}(K \log K + N_\gamma)$ operations per symbol. Compared to a CP-OFDM system that uses the IDFT and DFT but no pulse shaping, the complexity is increased by roughly $N_g + N_\gamma$ operations per symbol. For example, the complexity of a pulse-shaping MC system with $K = 1024$ carriers, symbol period $N = 1280$ ($TF = N/K = 1.25$), and pulse length $N_g = N_\gamma = 2N$ is only about 25% higher than that of a CP-OFDM system with the same K and N. We note that the overlap-add and pre-aliasing operations also require additional memory and introduce a latency of a few symbol periods.
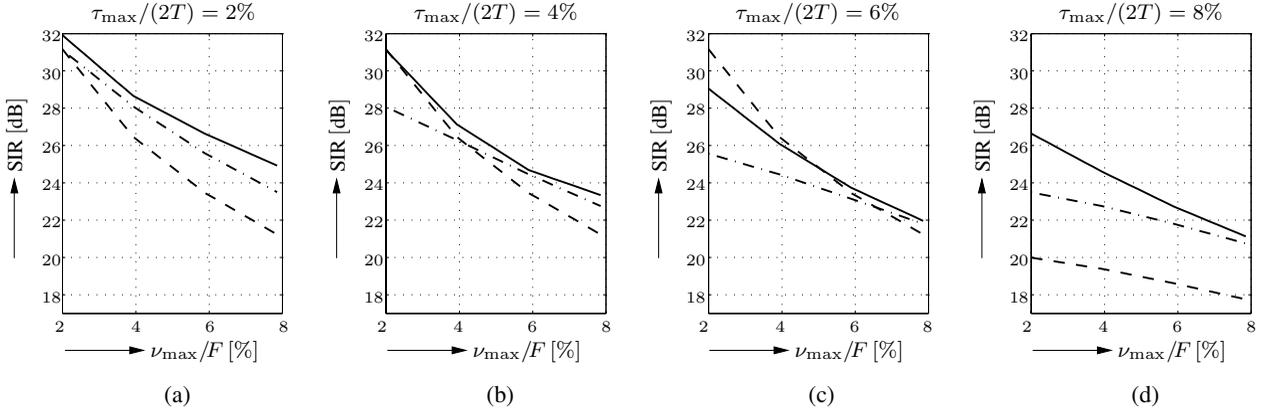
Fig. 2. *SIR versus normalized Doppler obtained with $\mathcal{S}_{cp}$ (dashed line), $\mathcal{S}_I$ (dash-dotted), and $\mathcal{S}_{II}$ (solid) in a DVB-T–like system for (a) $\tau_{max}/(2T) = 2\%$, (b) $\tau_{max}/(2T) = 4\%$, (c) $\tau_{max}/(2T) = 6\%$, (d) $\tau_{max}/(2T) = 8\%$.*
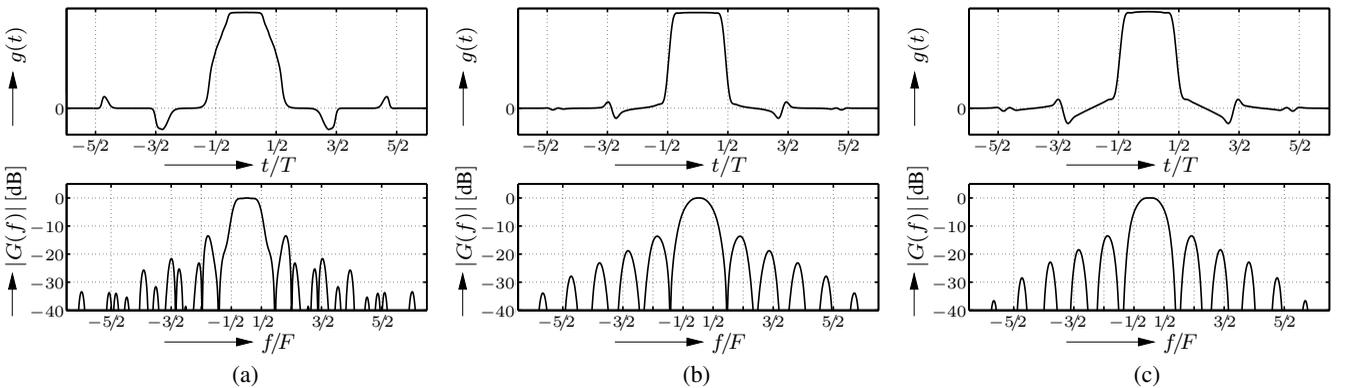

Fig. 3. *Pulse shape (top) and Fourier transform magnitude (bottom, in dB) of transmit pulses nonlinearly optimized for (a) $\tau_{max} = 20.83\,\mu s$, $\nu_{max} = 148\,Hz$, (b) $\tau_{max} = 62.5\,\mu s$, $\nu_{max} = 111\,Hz$, (c) $\tau_{max} = 83.33\,\mu s$, $\nu_{max} = 37\,Hz$.*

VIII. NUMERICAL RESULTS

To illustrate the potential of the pulse optimization techniques presented in Section VI, we provide some numerical results. All pulse designs were initialized using a truncated and orthogonalized version $g^\perp(t)$ of a Gaussian pulse that was chosen such that the ratio of its RMS duration and RMS bandwidth equals T/F (cf. [5, 18]). For the MC system obtained with the linear optimization method of Subsection VI-A, denoted $\mathcal{S}_I$, the orthogonalized Gaussian was used as the transmit pulse, i.e., $g^{(0)}(t) = g^\perp(t)$, and the optimal biorthogonal receive pulse was determined according to (22). For the system obtained with the nonlinear optimization of Subsection VI-B, denoted $\mathcal{S}_{II}$, $g^\perp(t)$ served as initialization for the transmit and receive pulses. We also compared our optimized designs with a conventional state-of-the-art CP-OFDM system (denoted $\mathcal{S}_{cp}$). The SIR, given by the reciprocal of (24), was used as a measure of performance.

A. DVB-T–like System

We first considered a DVB-T–like system operating at 800 MHz, with subcarrier separation $F = 2\,kHz$ and symbol period $T = 562.5\,\mu s$. We thus have $TF = 1.125$, corresponding to a redundancy of 12.5% and a spectral efficiency proportional to $1/(TF) = 0.89$. For the CP-OFDM system, this implies a CP length of $T_{cp} = 62.5\,\mu s$. We assumed WSSUS channels characterized by the brick-shaped scattering function (23) with maximum delay $\tau_{max} \in \{20.83\,\mu s, 31.25\,\mu s, 62.5\,\mu s, 83.33\,\mu s\}$ and maximum Doppler $\nu_{max} \in \{37\,Hz, 74\,Hz, 111\,Hz, 148\,Hz\}$. This corresponds to path lengths of up to 25 km and relative velocities of up to 200 km/h. Such scenarios might occur e.g. in single-frequency DVB-T networks providing digital video in high-speed trains.

The SIR obtained with the systems $\mathcal{S}_{cp}$, $\mathcal{S}_I$, and $\mathcal{S}_{II}$ is shown in Fig. 2 as a function of the normalized maximum Doppler ν_{max}/F for various normalized maximum delays τ_{max}/T (we note that the optimization was redone for each set of channel parameters τ_{max}, ν_{max}). As expected, the SIR of all systems decreases—i.e., there is more ISI/ICI—for increasing τ_{max} and ν_{max}, with the exception that the SIR of $\mathcal{S}_{cp}$ is independent of τ_{max} as long as $\tau_{max} \leq T_{cp}$. It is seen that $\mathcal{S}_I$ and, even more so, $\mathcal{S}_{II}$ outperform $\mathcal{S}_{cp}$ for a broad range of channel parameters. The gains are particularly pronounced for channels with large ν_{max} and small-to-medium τ_{max} (see Fig. 2(a) and (b)) as well as for channels with $\tau_{max} > T_{cp}$ (see Fig. 2(d)). Only for channels with τ_{max} slightly below T_{cp} and small ν_{max} is $\mathcal{S}_{cp}$ (slightly) superior to $\mathcal{S}_{II}$ (see Fig. 2(c)).

Fig. 3 shows the transmit pulse obtained with nonlinear numerical optimization (system $\mathcal{S}_{II}$) for channels with (τ_{max}, ν_{max}) equal to $(20.83\,\mu s, 148\,Hz)$, $(62.5\,\mu s, 111\,Hz)$, and $(83.33\,\mu s, 37\,Hz)$. It is seen that for large ν_{max}, the pulse tends to be more concentrated in frequency. This makes sense
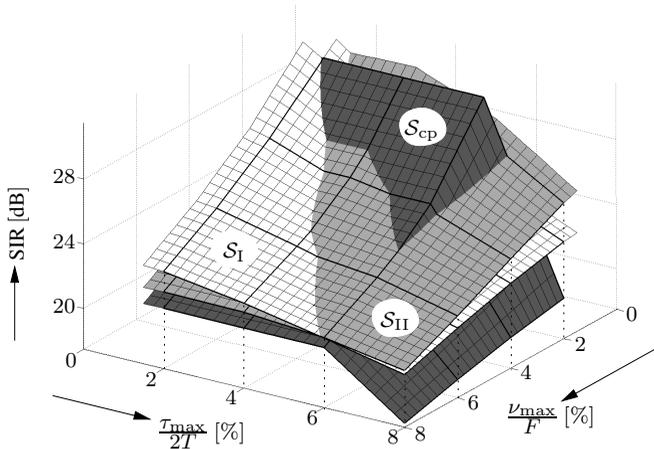
Fig. 4. *SIR versus maximum normalized delay and maximum normalized Doppler obtained with $\mathcal{S}_{\mathrm{cp}}$ (dark grey), $\mathcal{S}_{\mathrm{I}}$ (white), and $\mathcal{S}_{\mathrm{II}}$ (light grey). Here, $\mathcal{S}_{\mathrm{I}}$ and $\mathcal{S}_{\mathrm{II}}$ have been optimized for $\tau_{\max}/(2T) = \nu_{\max}/F = 6\%$.*

Fig. 5. *SIR achieved with $\mathcal{S}_{\mathrm{cp}}$, $\mathcal{S}_{\mathrm{I}}$, and $\mathcal{S}_{\mathrm{II}}$ using robustness modes A and C for DRM channels 2 and 5.*

because it means that the (large) Doppler shifts do not result in excessive ICI. In contrast, for large $\tau_{\max}$, the pulse is better concentrated in time such that the (large) delay spread does not result in excessive ISI.

To assess the robustness of our pulse designs to deviations of the true channel parameters from the nominal ones, we designed the systems $\mathcal{S}_{\mathrm{I}}$ and $\mathcal{S}_{\mathrm{II}}$ for $\tau_{\max} = 62.5\,\mu s$ and $\nu_{\max} = 111\,\mathrm{Hz}$ (i.e., $\tau_{\max}/(2T) = \nu_{\max}/F = 6\%$) and evaluated their SIR performance for various other values of $\tau_{\max}$ and $\nu_{\max}$. The results are shown as a 3-D plot in Fig. 4. Again, our designs $\mathcal{S}_{\mathrm{I}}$ and $\mathcal{S}_{\mathrm{II}}$ are superior to $\mathcal{S}_{\mathrm{cp}}$ except for the case where $\tau_{\max}$ is close to T_{cp} and, simultaneously, $\nu_{\max}$ is small. Furthermore, $\mathcal{S}_{\mathrm{II}}$ is seen to be superior to $\mathcal{S}_{\mathrm{I}}$ for $\tau_{\max}$ and $\nu_{\max}$ near the design parameters. This superiority is maintained for more dispersive channels (larger $\tau_{\max}$ or $\nu_{\max}$). However, for less dispersive channels, $\mathcal{S}_{\mathrm{I}}$ is less affected by the parameter mismatch.

B. DRM System

Next, we consider the application of our pulse optimization techniques to an MC system corresponding to the ETSI digital audio broadcasting standard *Digital Radio Mondial* (DRM) [37]. DRM specifies four so-called robustness modes A through D that correspond to CP-OFDM systems with different parameter sets, which are suited to channels with increasingly stronger time- and frequency-selective fading. For example, mode A (low redundancy, large spectral efficiency) is designed for almost no fading while mode D (high redundancy, small spectral efficiency) is intended for fading channels with severe delay and Doppler. For performance evaluation purposes, the DRM standard also specifies six channel models (1–6) with increasingly adverse time-frequency selectivity.

For robustness modes A and C and channels 2 and 5, Fig. 5 shows the SIR obtained with pulse-shaping MC systems that were designed using our optimization procedures, as well as the SIR obtained with the respective standardized CP-OFDM system. Robustness mode A uses a subcarrier separation of $F = 41\frac{2}{3}\,\mathrm{Hz}$, a symbol period of $T = 26\frac{2}{3}\,\mathrm{ms}$, and a CP length
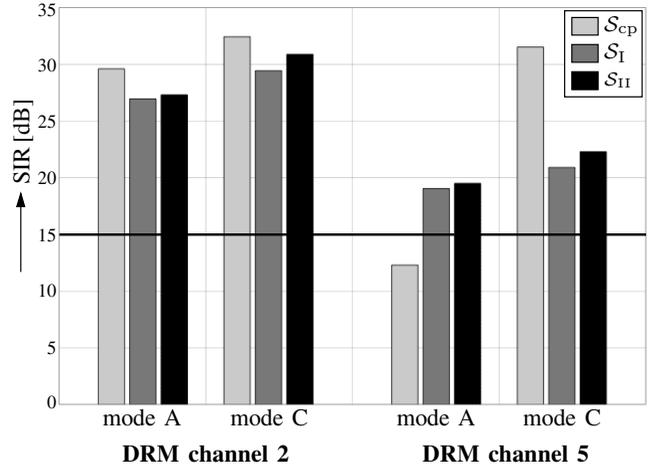
of $T_{\mathrm{cp}} = 2\frac{2}{3}\,\mathrm{ms}$, amounting to $TF = 10/9$, i.e., a redundancy of 11.1%. Robustness mode C uses $F = 3000/44\,\mathrm{Hz} \approx 68.2\,\mathrm{Hz}$, $T = 20\,\mathrm{ms}$, and $T_{\mathrm{cp}} = 5\frac{1}{3}\,\mathrm{ms}$, amounting to $TF = 15/11$, i.e., a redundancy of 36.4%. Assuming operation of the DRM systems at an SNR of $15\,\mathrm{dB}$, a target SIR larger than $15\,\mathrm{dB}$ is required to avoid performance limitation due to ISI/ICI. In the case of the mildly dispersive channel 2, all MC systems achieve SIRs of about $30\,\mathrm{dB}$, even in mode A with low redundancy. For the strongly dispersive channel 5, however, the standardized CP-OFDM system $\mathcal{S}_{\mathrm{cp}}$ achieves only $12.3\,\mathrm{dB}$ in mode A, i.e., almost $3\,\mathrm{dB}$ less than the target SIR. In this case, the CP-OFDM system would have to be switched to the less spectrally efficient mode C to achieve the target SIR. In contrast, both $\mathcal{S}_{\mathrm{I}}$ and $\mathcal{S}_{\mathrm{II}}$ achieve an SIR of about $19\,\mathrm{dB}$ even in mode A. We conclude that our optimized MC systems can be operated in the low-redundancy mode A even for adverse channels. For a DRM bandwidth of $10\,\mathrm{kHz}$, 64-QAM modulation, and a code rate of 0.6, this means that our designs support a data rate of $26.6\,\mathrm{kbit/s}$ instead of $16.6\,\mathrm{kbit/s}$ and thus allow a 60% increase in data rate (cf. [37, Annex H]). Similar observations apply to channel 6 (not shown). It should be noted that we used the DRM system parameters (lattice constants T, F) in our optimizations; additional gains could be achieved by an adaptation of the lattice constants.

IX. CONCLUSION

We presented exact and approximate expressions for the intersymbol/intercarrier interference (ISI/ICI) of pulse-shaping multicarrier (MC) systems transmitting over doubly dispersive fading channels. Our analysis demonstrated that to achieve low interference, the transmit and receive pulses should be jointly well localized in time and frequency and close to an orthogonal system (i.e., almost OFDM). The existence of such pulse pairs was shown by exploiting the Ron-Shen duality of Weyl-Heisenberg frames and Riesz bases to adapt recent mathematical results on Weyl-Heisenberg frames to the MC context.

We furthermore proposed two pulse optimization techniques that both aim at the minimization of the ISI/ICI power: a linear

technique that assumes one pulse to be given and optimizes the respective other pulse, and a nonlinear technique that performs a joint optimization of both pulses. Our numerical results showed that the resulting optimized pulse-shaping MC systems can significantly outperform conventional CP-OFDM systems for realistic spectral efficiencies and channel parameters. We also presented efficient digital implementations of pulse-shaping MC systems whose computational complexity is only slightly larger than that of conventional CP-OFDM systems.

The proposed optimized pulses yield additional benefits that cannot be discussed in detail in this paper. Their reduced out-of-band energy allows a larger number of subcarriers to be used while still respecting a prescribed spectral mask. The optimized pulses further result in improved robustness to a frequency offset (which acts like an additional Doppler shift). Finally, there is a gradual SIR decrease for increasing maximum delay $\tau_{\max}$ (instead of the abrupt SIR decrease observed for $\tau_{\max} > T_{\mathrm{cp}}$ with CP-OFDM systems), which has the potential to obviate the need for time-domain equalizers in the case of very large delay spreads.

ACKNOWLEDGMENT

REFERENCES

[1] R. W. Chang, "Synthesis of band-limited orthogonal signals for multi-channel data transmission," *Bell Syst. Tech. J.*, vol. 45, pp. 1775–1796, Dec. 1966.

[2] A. Peled and A. Ruiz, "Frequency domain data transmission using reduced computational complexity algorithms," in *Proc. IEEE ICASSP-80*, pp. 964–967.

[3] L. J. Cimini, "Analysis and simulation of a digital mobile channel using orthogonal frequency division multiplexing," *IEEE Trans. Commun.*, vol. 33, pp. 665–675, July 1985.

[4] P. Smulders, "Exploiting the 60 GHz band for local wireless multimedia access: prospects and future directions," *IEEE Commun. Mag.*, vol. 40, no. 1, pp. 140–147, Jan. 2002.

[5] W. Kozek and A. F. Molisch, "Nonorthogonal pulseshapes for multicarrier communications in doubly dispersive channels," *IEEE J. Sel. Areas Commun.*, vol. 16, pp. 1579–1589, Oct. 1998.

[6] P. K. Remvik and N. Holte, "Carrier frequency offset robustness for OFDM systems with different pulse shaping filters," in *Proc. IEEE GLOBECOM-97*, pp. 11–15.

[7] A. Vahlin and N. Holte, "Optimal finite duration pulses for OFDM," *IEEE Trans. Commun.*, vol. 4, pp. 10–14, Jan. 1996.

[8] R. Haas and J. C. Belfiore, "A time-frequency well-localized pulse for multiple carrier transmission," *Wireless Personal Commun.*, vol. 5, pp. 1–18, 1997.

[9] H. Bölcskei, "Efficient design of pulse shaping filters for OFDM systems," in *Proc. SPIE Wavelet Applications in Signal and Image Processing VII 1999*, pp. 625–636.

[10] T. Strohmer and S. Beaver, "Optimal OFDM design for time-frequency dispersive channels," *IEEE Trans. Commun.*, vol. 51, pp. 1111–1122, July 2003.

[11] P. Siohan, C. Siclet, and N. Lacaille, "Analysis and design of OFDM/OQAM systems based on filterbank theory," *IEEE Trans. Signal Processing*, vol. 50, pp. 1170–1183, May 2002.

[12] H. Bölcskei, P. Duhamel, and R. Hleiss, "Orthogonalization of OFDM/OQAM pulse shaping filters using the discrete Zak transform," *Signal Processing*, vol. 83, pp. 1379–1391, July 2003.

[13] H. Bölcskei, P. Duhamel, and R. Hleiss, "Design of pulse shaping OFDM/OQAM systems for high data-rate transmission over wireless channels," in *Proc. IEEE ICC-99*, pp. 559–564.

[14] W. Kozek, G. Pfander, and G. Zimmermann, "Perturbation stability of coherent Riesz systems under convolution operators," *Applied and Computational Harmonic Analysis*, vol. 12, pp. 286–308, 2002.

[15] D. Schafhuber, G. Matz, and F. Hlawatsch, "Pulse-shaping OFDM/BFDM systems for time-varying channels: ISI/ICI analysis, optimal pulse design, and efficient implementation," in *Proc. IEEE PIMRC-02*, pp. 1012–1016.

[16] G. Matz, K. Gröchenig, F. Hlawatsch, A. Klotz, G. Tauböck, and A. Skupch, "Advanced mathematical models for the design and optimization of low-interference wireless multicarrier systems," in *Proc. MATHMOD 2006*, pp. 3.1–3.9.

[17] B. R. Saltzberg, "Performance of an efficient parallel data transmission system," *IEEE Trans. Commun. Technol.*, vol. 15, pp. 805–811, Dec. 1967.

[18] B. LeFloch, M. Alard, and C. Berrou, "Coded orthogonal frequency division multiplex," *Proc. IEEE*, vol. 83, pp. 982–996, June 1995.

[19] T. Strohmer, "Approximation of dual Gabor frames, window decay, and wireless communications," *Applied and Computational Harmonic Analysis*, vol. 11, no. 2, pp. 243–262, 2001.

[20] P. Jung and G. Wunder, "Iterative pulse shaping for Gabor signaling in WSSUS channels," in *Proc. IEEE-SP Workshop on Signal Processing Advances in Wireless Communications 2004*, pp. 368–372.

[21] K. Gröchenig and M. Leinert, "Wiener's lemma for twisted convolution and Gabor frames," *J. Amer. Math. Soc.*, vol. 17, no. 1, pp. 1–18, 2004.

[22] K. Gröchenig, *Foundations of Time-Frequency Analysis*. Boston: Birkhäuser, 2001.

[23] P. A. Bello, "Characterization of randomly time-variant linear channels," *IEEE Trans. Commun. Syst.*, vol. 11, pp. 360–393, 1963.

[24] J. G. Proakis, *Digital Communications*. New York: McGraw-Hill, 3rd ed., 1995.

[25] G. Matz and F. Hlawatsch, "Time-frequency characterization of random time-varying channels," in *Time-Frequency Signal Analysis and Processing: A Comprehensive Reference* (B. Boashash, ed.), ch. 9.5, pp. 410–419. Oxford (UK): Elsevier, 2003.

[26] W. Kozek and A. F. Molisch, "On the eigenstructure of underspread WSSUS channels," in *Proc. IEEE Workshop on Signal Processing Advances in Wireless Communications 1997*, pp. 325–328.

[27] A. Ron and Z. Shen, "Weyl-Heisenberg frames and Riesz bases in $L_2(\mathbb{R}^d)$," *Duke Math. J.*, vol. 89, no. 2, pp. 237–282, 1997.

[28] A. J. E. M. Janssen, "Duality and biorthogonality for Weyl-Heisenberg frames," *J. Fourier Analysis and Applications*, vol. 1, no. 4, pp. 403–436, 1995.

[29] T. Strohmer, "Numerical algorithms for discrete Gabor expansions," in *Gabor Analysis and Algorithms: Theory and Applications* (H. G. Feichtinger and T. Strohmer, eds.), ch. 8, pp. 267–294. Boston: Birkhäuser, 1998.

[30] K. Seip and R. Wallstén, "Density theorems for sampling and interpolation in the Bargmann-Fock space. II," *J. Reine Angew. Math.*, vol. 429, pp. 107–113, 1992.

[31] Y. Li and L. Cimini, "Bounds on the interchannel interference of OFDM in time-varying impairments," *IEEE Trans. Commun.*, vol. 49, pp. 401–404, March 2001.

[32] C. H. Wilcox, "The synthesis problem for radar ambiguity functions," in *Radar and Sonar, Part I* (R. E. Blahut, W. Miller, Jr., and C. H. Wilcox, eds.), pp. 229–260. New York: Springer, 1991.

[33] R. Tolimieri and R. S. Orr, "Characterization of Weyl-Heisenberg frames via Poisson summation relationships," in *Proc. IEEE ICASSP-92*, pp. 277–280.

[34] T. Pollet, M. V. Bladel, and M. Moeneclaey, "BER sensitivity of OFDM systems to carrier frequency offset and Wiener phase noise," *IEEE Trans. Commun.*, vol. 43, pp. 191–193, Feb. 1995.

[35] http://www.mathworks.com/access/helpdesk/help/toolbox/optim.

[36] P. P. Vaidyanathan, *Multirate Systems and Filter Banks*. Englewood Cliffs, NJ: Prentice Hall, 1993.

[37] ETSI, "Digital radio mondiale (DRM): system specification," EN 201 980, V2.1.1, 2004 (http://www.etsi.org).

Gerald Matz received the Dipl.-Ing. and Dr. techn. degrees in electrical engineering and the habilitation degree for "Communication Systems" from Vienna University of Technology, Austria, in Dec. 1994, Dec. 2000, and Sept. 2004, respectively. Since Jan. 1995 he has been with the Department of Communications and Radio-Frequency Engineering, Vienna University of Technology where he currently holds a tenured position as Associate Professor. From March 2004 to Feb. 2005 he was on leave as an Erwin Schrödinger Fellow with the Laboratoire des Signaux et Systèmes, Ecole Supérieure d'Electricité (France).

Prof. Matz has directed or actively participated in several research projects funded by the Austrian Science Fund (FWF) and by the European Union.

He has published some 80 papers in international journals, conference proceedings, and edited books. He serves as Associate Editor of the *IEEE Transactions on Signal Processing* and the *IEEE Signal Processing Letters*, was Technical Program Co-Chair of the 12th European Signal Processing Conference, and member of the Program Committee of numerous IEEE conferences. In 2006, he received the Kardinal Innitzer Most Promising Young Investigator Award. His research interests include wireless communications, statistical signal processing, and information theory.

Dieter Schafhuber received the Dipl.-Ing. and Dr. techn. degrees in electrical engineering from Vienna University of Technology, Vienna, Austria, in 1999 and 2004, respectively. Since 2004, he has been with BMW Group, Munich, Germany. His research interests are in the areas of wireless communications and statistical signal processing.

Karlheinz Gröchenig is Professor of Mathematics at the University of Vienna. From 1988 until 2004 he was Professor at the University of Connecticut, where he was awarded tenure in 1993 and promoted to Full Professor in 1998. He is recipient of a Marie-Curie Excellence Grant of the European Community and team leader of the European Center for Time-Frequency Analysis. His field of research is harmonic analysis, operator theory, and sampling theory with applications in signal analysis and wireless communications. He is author of the book "Foundations of Time-Frequency Analysis" and of 100 research articles.

Manfred Hartmann received the Dipl.-Ing. degree in Electrical Engineering from Vienna University of Technology, Austria, in Apr. 2003. From May 2003 till Dec. 2004 he has been with the Department of Communications and Radio-Frequency Engineering, Vienna University of Technology, working as a Research Assistant within the project "Advanced Multicarrier Systems for Wireless Communications." Since March 2005 he is with Austrian Research Centers GmbH - ARC, Vienna. His research interests include statistical signal processing, wireless communications, and biomedical signal processing.

Franz Hlawatsch received the Diplom-Ingenieur, Dr. techn., and Univ.-Dozent (habilitation) degrees in electrical engineering/signal processing from Vienna University of Technology, Vienna, Austria in 1983, 1988, and 1996, respectively.

Since 1983, he has been with the Institute of Communications and Radio-Frequency Engineering, Vienna University of Technology, where he holds an Associate Professor position. During 1991-1992, as a recipient of an Erwin Schrödinger Fellowship, he spent a sabbatical year with the Department of Electrical Engineering, University of Rhode Island, Kingston, RI. In 1999, 2000, and 2001, he held one-month Visiting Professor positions with INP/ENSEEIHT/TeSA, Toulouse, France and IRCCyN, Nantes, France. He (co)authored a book, a review paper that appeared in the *IEEE Signal Processing Magazine*, about 150 refereed scientific papers and book chapters, and two patents. He coedited two books. His research interests include signal processing for wireless communications, nonstationary statistical signal processing, and time-frequency signal processing.

Prof. Hlawatsch was Technical Program Co-Chair of EUSIPCO 2004 and served on the technical committees of numerous IEEE conferences. He is currently serving as an Associate Editor for the *IEEE Transactions on Signal Processing* and as a member of the IEEE SPCOM Technical Committee. He is coauthor of a paper that won an IEEE Signal Processing Society Young Author Best Paper Award.